

Theoretical Analysis and Novel Simulation for Single Shunt Rectifiers

TAKASHI HIRAKAWA^{id}, (Student Member, IEEE),
AND NAOKI SHINOHARA^{id}, (Senior Member, IEEE)

RISH, Kyoto University, Uji 611-0011, Japan

Corresponding author: Takashi Hirakawa (takashi_hirakawa@rish.kyoto-u.ac.jp)

This work was supported in part by the Strategic Innovation Promotion Project by Japan Science and Technology Agency (JST).

ABSTRACT Rectifiers are essential for microwave wireless power transfer (MWPT). RF-DC conversion efficiency must be improved for the practical use of MWPT. The focus of this research is related to single shunt rectifiers. Former research explained the operations of single shunt rectifiers in the frequency domain. Currently, we are using a harmonic balance method for the circuit simulations. These analyses focus on the frequency domain and transient phenomena were not directly analyzed. Also, the differences between experiments and their simulations are still issues in designing rectifiers. Therein, we analyzed an ideal rectifier with transient analysis and simulation. We also propose a novel simulation for single shunt rectifiers. Our simulation method is based on simple theories focusing on the steady-state condition of transient phenomena. In our analysis method, the output DC voltage is a fixed parameter and the DC current with the voltage is calculated. Therefore, this method is suitable for analyzing I-V characteristics. First, theoretical solutions are compared with Advanced Design System (ADS) simulations and they show the good agreement. Next, we created the novel simulation with our analysis method. Their results are also compared with ADS simulations. These analyses showed good agreement. Therefore, our novel method is consistent with former researches and commercial simulations. As a result, this research shows a novel analysis method for single shunt rectifiers and its consistency.

INDEX TERMS Rectifiers, circuit analysis, circuit simulation, current-voltage characteristics, energy efficiency, circuit optimization, microwave circuits, microwave theory and techniques.

I. INTRODUCTION

IoT society needs a large number of sensors and batteries. Microwave wireless power transfer (MWPT) can reduce the batteries and flexible construction of sensor networks. MWPT have been improved [1]. MWPT consists of oscillators, antennas, and rectifiers, where the focus of this research is on rectifiers.

RF-DC conversion efficiency should be improved for the practical use of MWPT. To design high-efficiency rectifiers, the modeling, simulation, and analytical calculation methods have been improved [2]–[4]. Also, general characteristics of rectifiers have been studied with the concentrated circuit and floating equation [5]–[7].

Analytical models and effects of the class-F output filter are still under investigation [8]–[11]. Also, recent research shows the novel method with closed-form expressions [12],

The associate editor coordinating the review of this manuscript and approving it for publication was Hiu Yung Wong^{id}.

[13]. These research are based on the former research [6], [7]. However, these studies are based on harmonic analysis and transient phenomena are not analyzed in detail. Herein, we analyzed the transient operation of an ideal single shunt rectifier and revealed its RF-DC conversion efficiency characteristics. In addition, we produced the new circuit simulation for single shunt rectifiers and analyzed their characteristics by our simulations.

II. ANALYSIS METHODS FOR RECTIFIERS

In this section, we describe ideal single shunt rectifiers and their analysis. Furthermore, a comparison of simulation methods for rectifiers is shown.

A. TRADITIONAL ANALYSIS

Fig. 2 shows the schematics of the ideal single shunt rectifier. This rectifier includes a transmission line before the parallel connected diode and its length is a quarter wavelength of the

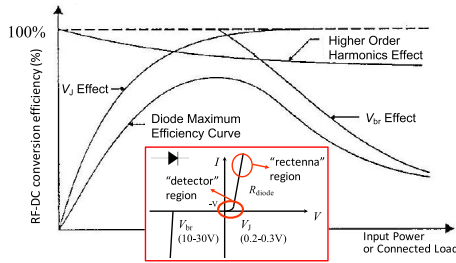


FIGURE 1. RF-DC conversion efficiency of rectifiers [7].

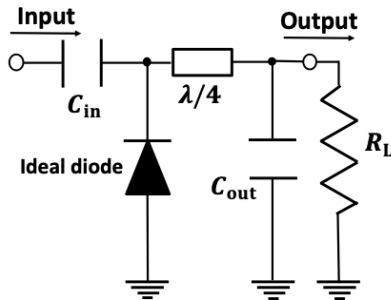


FIGURE 2. Ideal single shunt rectifier.

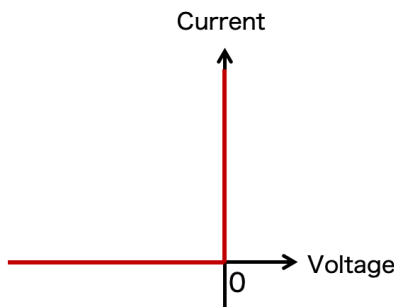


FIGURE 3. Characteristics of ideal diode.

input sinusoidal wave. Without $\lambda/4$ -length line, this circuit works as same as clamper circuits. But the transmission line makes this circuit a full-wave rectifier. In this rectifier, an ideal diode is connected and its I-V characteristic is shown in Fig. 3. This is the same as an ideal switch and no losses are generated at the diode. Traditional research claims that this transmission line length and the output capacitor C_{out} satisfy the ideal working condition of rectifiers. The condition is shown in below ([5]):

$$Z_n = 0 \text{ (} n = \text{even) , } \infty \text{ (} n = \text{odd) .} \quad (1)$$

Z_n indicates the apparent impedance of output loads from the diode-connected point. Such kinds of impedance differ for each harmonic and n means the harmonic order. Certainly, a quarter-wavelength transmission line and an ideal capacitance satisfy the above condition. This condition is assumed that the return wave is a pulse wave with the ideal condition, and the current wave is full-wave rectified as shown in Fig. 4. Also, the previous research claims the RF-DC conversion efficiency of the rectifier with such condition equals to 100 %.

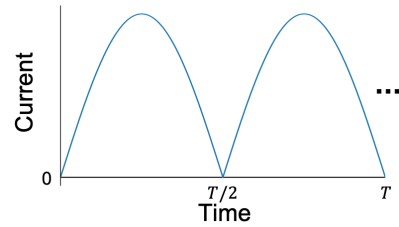


FIGURE 4. Full-wave rectified current.

TABLE 1. Comparison between each method.

Fixed parameter	HB [14]	Transient [15]	Our method
Output	Resistance	Resistance	Voltage
Speed	Power	Voltage	Current
Accuracy	Rapid	Slow	Middle
Generality	High	High	Same as transient
	General	General	For single shunt

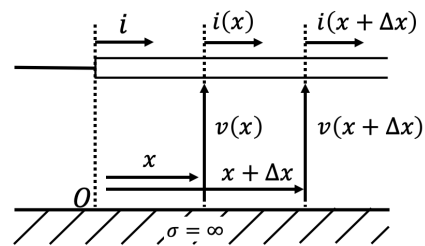


FIGURE 5. Model of transmission lines.

B. SIMULATION METHODS

Harmonic balance (HB) and transient methods are traditional and prevalent simulations for microwave rectifiers. HB simulations are rapid and accurate for solving the periodic problem. But, its accuracy is depending on the number of harmonics. When we design a rectifier, we usually use a HB simulation because of its rapidness. Also, we use a transient simulation for obtaining the detail operation of a designed rectifier. Therein, we produced a novel simulation method with middle speed and accuracy for single shunt rectifiers. However, our method shows deficiencies related to its generality. A comparison among the three methods are shown in Tab. 1. We show the method and analyzed results in the next section.

III. ANALYSIS OF THE SINGLE SHUNT RECTIFIER

A. PROPAGATION IN STRIP LINES

Fig. 5 shows an ideal transmission line. Kirchhoff's laws lead the following equations (2) and (3).

$$v - \left(v + \frac{\partial v}{\partial x} \Delta x \right) = (R \Delta x) i + (L \Delta x) \frac{\partial i}{\partial t}, \quad (2)$$

$$i - \left(i + \frac{\partial i}{\partial x} \Delta x \right) = (G \Delta x) v + (C \Delta x) \frac{\partial v}{\partial t}, \quad (3)$$

R, L, G, C indicate the linear densities of resistance, inductance, conductance, and capacitance respectively. The

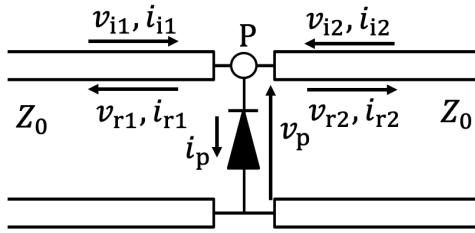


FIGURE 6. Model of the diode connected transmission line.

next solutions are obtained with the non-loss condition $R = G = 0$.

$$v(x, t) = f_i(x - \beta t) + f_r(x + \beta t), \quad (4)$$

$$i(x, t) = \frac{1}{Z_0} (f_i(x - \beta t) - f_r(x + \beta t)). \quad (5)$$

Equations (4) and (5) are the general solutions of wave propagation. f_i and f_r are arbitrary functions and Z_0 is a characteristic impedance of the transmission line. Functions $f_i(x - \beta t)$ and $f_r(x + \beta t)$ respectively mean the incident (forward) and the reflected (backward) wave, respectively. β indicates the propagation velocity and is equal to $1/\sqrt{LC}$. These equations are fundamental and necessary for the theoretical transient analysis.

B. REFLECTION AT THE DIODE-CONNECTED POINT

Single shunt rectifiers include the parallel connected diode. Therein, we consider the circuit as shown in Fig. 6. Incident and reflection waves in Fig. 6 should be calculated for analyzing the transient operation. Equations (6 - 9) show the boundary conditions in Fig. 6.

$$v_{i1} + v_{r1} = v_{i2} + v_{r2} = v_p \quad (6)$$

$$i_{i1} + i_{r1} = i_{i2} + i_{r2} + i_p \quad (7)$$

$$i_{i1} = \frac{1}{Z_0} v_{i1}, \quad i_{r1} = -\frac{1}{Z_0} v_{r1} \quad (8)$$

$$i_{i2} = -\frac{1}{Z_0} v_{i2}, \quad i_{r2} = \frac{1}{Z_0} v_{r2} \quad (9)$$

Herein, the connected diode is an ideal diode and $v_p - i_p$ characteristics are shown in Fig. 3. Equations (4) and (5) derive the following ones.

$$v_p = v_{i1} + v_{i2}, \quad i_p = 0 \quad (0 \leq v_{i1} + v_{i2}), \quad (10)$$

$$v_p = 0, \quad i_p = \frac{2}{Z_0} (v_{i1} + v_{i2}) \quad (0 > v_{i1} + v_{i2}). \quad (11)$$

Next, we consider the DC voltage. With DC voltage, Eq. (6) is changed to Eq. (12).

$$v_{i1} + v_{r1} = v_{i2} + v_{r2} = v_p - V_{DC} \quad (12)$$

The output DC voltage is defined as V_{DC} . This characteristic derives Eqs. (13) and (14).

$$v_p = v_{i1} + v_{i2}, \quad i_p = 0 \quad (-V_{DC} \leq v_{i1} + v_{i2}), \quad (13)$$

$$v_p = 0, \quad i_p = \frac{2}{Z_0} (v_{i1} + v_{i2} + V_{DC}) \quad (-V_{DC} > v_{i1} + v_{i2}). \quad (14)$$

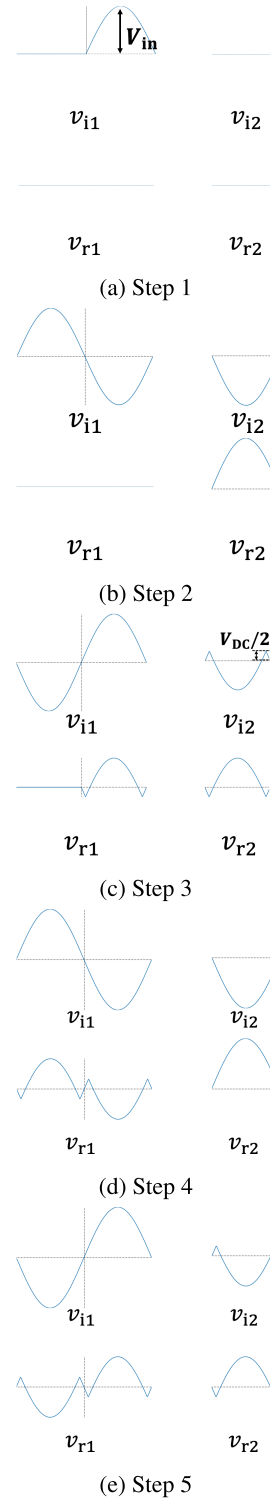


FIGURE 7. Calculated wave form.

These equations show the reflection at the diode-connected point. We can obtain the waveform of v_{i1} , v_{i2} , v_{r1} , v_{r2} , v_p , and i_p with Eqs. (13) and (14). This calculation is conducted in steps of half a period each.

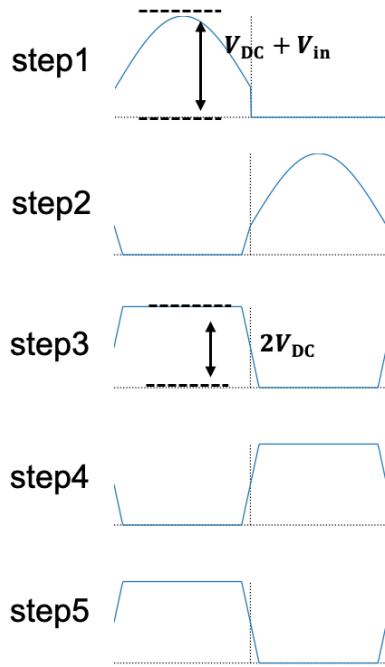


FIGURE 8. Calculated v_p .

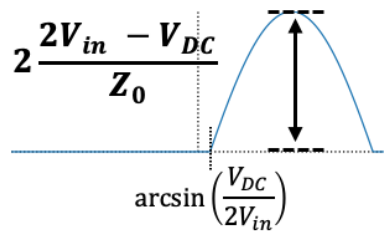


FIGURE 9. i_p vs time at the steady state.

Figs. 7 and 8 show the waveform at each half period. The step indicates the number of the half period. Herein, V_{in} is the amplitude of an incident wave. These figures show that the wave forms at steps 3 and 5 are the same. This indicates the wave form at step 5 is that at the steady state and we can solve the steady-state operation. Fig. 9 shows the current change at the steady state. We can calculate the averaged current from Fig. 9 and it is expressed by Eq. (15).

$$\bar{i}_p = \frac{1}{\pi} \int_{\arcsin\left(\frac{V_{DC}}{2V_{in}}\right)}^{\frac{\pi}{2}} \frac{2}{Z_0} (2V_{in} \sin \theta - V_{DC}) d\theta. \quad (15)$$

When C_{out} is an ideal capacitor, the output DC current is equal to \bar{i}_p . In this case, Eq. (16) is calculated by Eq. (15).

$$V_{DC} = \frac{2Z_L}{\pi Z_0} \int_{\arcsin\left(\frac{V_{DC}}{2V_{in}}\right)}^{\frac{\pi}{2}} \frac{2}{Z_0} (2V_{in} \sin \theta - V_{DC}) d\theta. \quad (16)$$

Herein, we define the normalized value as follows.

$$\hat{V} = \frac{V_{DC}}{V_{in}}, \quad (17)$$

$$\hat{z} = \frac{R_L}{Z_0}. \quad (18)$$

$$\hat{I} = \frac{\hat{V}}{\hat{z}} = \frac{I_{DC}}{V_{in}/Z_0}. \quad (19)$$

$$\eta_{DC} = 2\hat{V}^2/\hat{z} = 2\hat{I}^2\hat{z} = 2\hat{I}\hat{V}. \quad (20)$$

Eqs. (16 - 18) can be used to derive Eq. (21).

$$\frac{4}{\pi} \sqrt{1 - \frac{\hat{V}^2}{4}} + \frac{2}{\pi} \hat{V} \arcsin\left(\frac{\hat{V}}{2}\right) - \hat{V} = \frac{\hat{V}}{\hat{z}} \quad (21)$$

We cannot obtain the analytical solution of \hat{V} from Eq. (15), but this equation can be easily solved by computer simulations. Also, Fig. 9 is different from Fig. 4 and does not seem to be a full-wave rectification. However, the maximum value is expressed by $2(2V_{in} - V_{DC})/Z_0$ and this means double-current rectification. This indicates single shunt rectifiers are similar to the double-current rectifier circuits and the output wave is not like Fig. 4. The key point of the operation is a reflection by C_{out} . In this circuit, only a positive voltage part of the input sinusoidal wave is reflected and converted to negative voltage wave. With a 90-degree line, the reflected wave is inputted to the diode at the same time that a negative voltage part is input to the diode. Both negative voltage waves generate a diode current as shown in Fig. 9. This is because single shunt rectifiers work as double-current rectifiers. When the length of the transmission line is not 90 degrees, the interference between the reflected negative voltage wave and input positive wave occurs at the diode-connected point in some part of the period. This makes RF-DC conversion efficiency decrease. The former explanations are the reason that an ideal single shunt rectifier needs a 90-degree line and an output capacitance. Also, this output filter satisfies Eq. (1). In [5], this condition is explained by focusing on harmonics phenomena. This paper explains the appropriate conditions for transient phenomena. On the other hand, we have revealed the detailed operation including I-V characteristics of an ideal single shunt rectifier and proposed a novel analytical method. Our method is adoptable for computer simulations and that is shown in the next section.

C. THEORETICAL ANALYSIS METHOD FOR A SINGLE SHUNT RECTIFIER

In Sec. III-B, we theoretically solved the operation of an ideal single shunt rectifier. In the deriving process, we tried the iterative calculation method and judged the steady state by the congruency of wave forms at each steps. Iterative calculation and calculations of congruencies are suitable for computer simulations. Therein, we created the simulation program for simple single shunt rectifiers (Fig. 10) with Python language. The flowchart of our program is shown in Fig. 11. Fig. 10 includes a note for an input filter. This is used as a matching circuit traditionally. With a stub, the through and reflection wave is calculated as follows.

$$V_r = \Gamma_{input} V_{in} \quad (22)$$

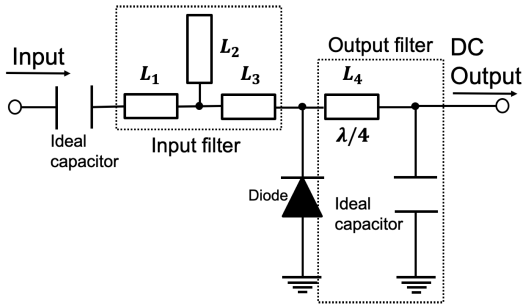


FIGURE 10. Programmed circuit.

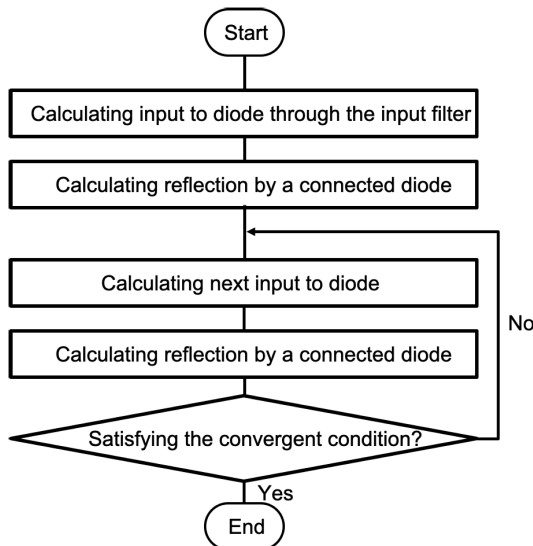


FIGURE 11. Flowchart of program.

$$\Gamma_{\text{input}} = \Gamma_{\text{in}} + \alpha \sum_{i=0}^{\infty} \Gamma_{\text{stub}}^i H\left(t - \frac{2L(i+1)}{v}\right) \exp^{-2(i+1)kLj} \quad (23)$$

$$\alpha = (\Gamma_{\text{in}} + 1)(\Gamma_{\text{stub}} + 1) \quad (24)$$

$$\Gamma_{\text{in}} = -\frac{1}{1 + 2\widehat{Z}_{\text{stub}}} \quad (25)$$

$$\Gamma_{\text{stub}} = \frac{1 - 2\widehat{Z}_{\text{stub}}}{1 + 2\widehat{Z}_{\text{stub}}} \quad (26)$$

Herein, H is a Heaviside step function and the time $t = 0$ indicates that an incident wave just reached to the stub connected point. Eq. (23) includes an infinity series. In our simulation, the calculated terms are ten and $\widehat{Z}_{\text{stub}}$ is equal to 1. Thus, an actual equation in our simulation is Eq. (27)

$$\Gamma_{\text{input}} = -\frac{1}{3} + \frac{4}{9} \sum_{i=0}^9 \left(-\frac{1}{3}\right)^i H\left(t - \frac{2L(i+1)}{v}\right) \times \exp^{-2(i+1)kLj} \quad (27)$$

The above equations derives the wave reflection at the input filter. Also, Eqs. (6) to (9) and I-V equations can derive the reflection by the connected diode. I-V characteristics of

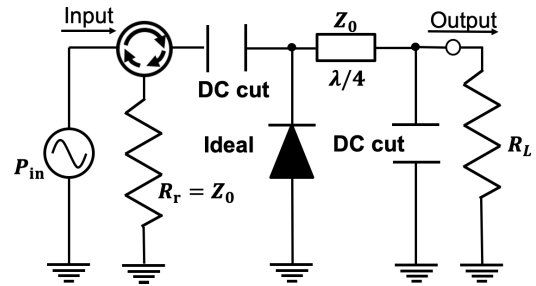


FIGURE 12. Simulated circuit with ADS.

TABLE 2. Diode parameters in the simulation.

Diode parameters	values
Saturation current I_s	0.1 fA
Series resistance R_s	0 Ω
Diffusion capacitance C_d	0 F
Junction capacitance C_{j0}	0 F
Breakdown voltage B_{rvmv}	1×10^7
N	1×10^{-4}

TABLE 3. Simulation parameters.

Simulation parameters	values
Input power P_{in}	10 mW
Characteristic impedance Z_0	50 Ω
Basic frequency f	2.45 GHz
Load resistance R_L	From 0.1 Ω to 100 k Ω

diodes are nonlinear. With computer simulation, their solution can be obtained by numerical methods. The reflection by a shunt-connected ideal capacitance is a short-end reflection. From the above discussion, we can calculate all reflections. These calculations and the method shown by Fig. 11 derives the operation of the rectifier at the steady state.

IV. THE OPERATION OF AN IDEAL SINGLE SHUNT RECTIFIER

A. SIMULATIONS WITH A COMMERCIAL APPLICATION

We used ADS (Advanced Design System) to simulate an ideal single shunt rectifier. The simulation circuit is composed as shown in Fig. 12. With an ideal diode, this circuit is the same one as Fig. 2. Diode parameters are shown in Tab. 2. With the spice model, an ideal diode characteristics cannot be simulated perfectly, so we have set parameters to imitate that. Other parameters are shown in Tab. 3. We set P_{in} as 10 mW because the incident voltage amplitude equals to 1 V with 50 - Ω characteristic impedance. These parameter settings are just for the simplification of results. This simulation is conducted with an ideal condition. Herein, the operation depends on the normalized constants, and these values as shown in Tab. 3 have no effect. The HB method is used for this analysis and considered harmonics up to the 30th frequency.

B. ANALYSIS OF AN IDEAL SINGLE SHUNT RECTIFIER

We solved Eq. (21) by changing \widehat{Z} from $10^{-2.7}$ to $10^{3.3}$ logarithmically and simulated the circuit (Fig. 12) with the condition as shown in Tab. 3. Figs. 13 and 14 show the comparison

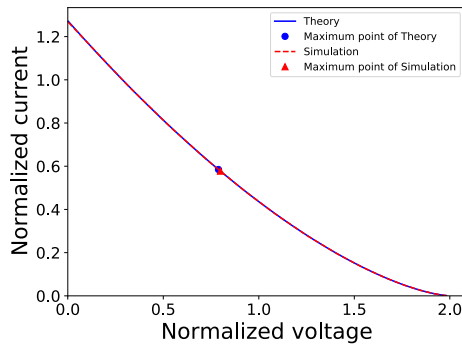


FIGURE 13. Relationship between current and voltage.

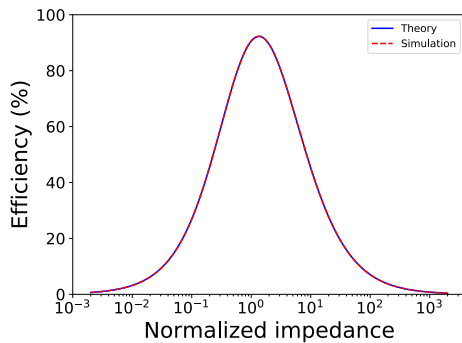


FIGURE 14. RF-DC conversion efficiency depending on the load impedance.

between the theoretical and simulation results. The blue and orange lines indicate the theoretical solutions and the simulation results, respectively. Both figures show the good agreement. Fig. 13 shows the *i-v* characteristics of an ideal single shunt rectifier. This figure shows the monotonically decreasing. The blue and red points indicate the maximum efficiency condition in the theoretical and simulation results, respectively. The normalized current and voltage at the blue point were 0.585 and 0.789, respectively. On the other hand, the normalized current and voltage at the red point were 0.578 and 0.799, respectively. Maximum voltages of blue and orange lines are 1.982 and 1.983, respectively. Maximum currents of the same are 1.271 and 1.267, respectively. Fig. 14 shows the characteristics of RF-DC conversion efficiency. Herein, these circuits include no lossy components and the operation is consist of reflection and RF-DC conversion. Therefore, the sum of reflection ratio and RF-DC conversion efficiency is equal to 100%. The maximum efficiencies of theoretical calculation and simulation were 92.26% and 92.30%, respectively. The normalized impedances at the maximum efficiency conditions were 1.35 and 1.38, respectively.

These figures show the good validity of the Eq. (21). Considering the current wave (Fig. 9), we can calculate the maximum voltage and current. With $V_{DC} = 2V_{in}$, the amplitude of i_p equals to 0 and also DC current equals to zero. Therefore, theoretical maximum normalized voltage is just two. With $V_{DC} = 0$, Eq. (15) takes the maximum value and its value is $4V_{in}/\pi Z_0$. Therefore, the theoretical maximum nor-

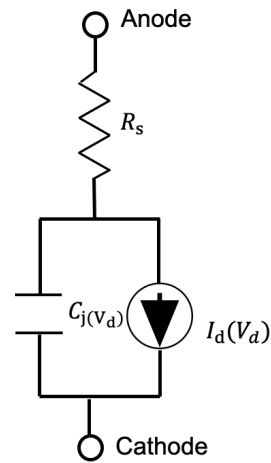


FIGURE 15. Equivalent circuit for a diode.

malized current is $4/\pi = 1.273$. These values are consistent with Fig. 13. Without any stubs, a single shunt rectifier has limits as their values. Fig. 14 shows interesting characteristics with high load impedance. Former research concluded that the decrease in RF-DC conversion efficiency with high load impedance occurs by the breakdown of diodes. Our analytical results, which are consistent with the simulation results, contradict the preceding studies. This indicates harmonic analysis or floating equations, which has been primarily used in previous research, are not enough for the analysis of rectifier operations. Also, it was indicated that the RF-DC conversion efficiency decrease is just a characteristics of single shunt rectifier. On the other hand, this circuit include no stubs. With a stub for an input filter, we can reduce reflection and improve the RF-DC conversion efficiency. Herein, we may obtain the characteristics as shown in former research. We will discuss this problem in the next section.

V. CONSISTENCY WITH THE COMMERCIAL SIMULATOR

In the previous section, we show the basic operation of an ideal single shunt rectifier and our analysis method. Next, we confirmed the consistency between our simulation program and ADS.

A. SIMULATION CONDITION

We used a simple equivalent circuit for diodes as shown in Fig. 15. The connected diode has characteristics as shown in Fig. 3. This circuit is also used in previous research and analysis [6]. We focused on *i-v* characteristics of single-shunt rectifiers. We also optimized the input filter (L_2 and L_3) in Fig. 10 with the differential evolution method. This optimization increased the output DC current to its maximum value. Herein, our program is run with a fixed output DC voltage as shown in Sec. III. Therefore, improving RF-DC conversion efficiencies means the same as improving DC output current and the rectifier obtains the maximum RF-DC conversion efficiency with the optimized input filter. These optimizations are conducted with each output DC voltages.

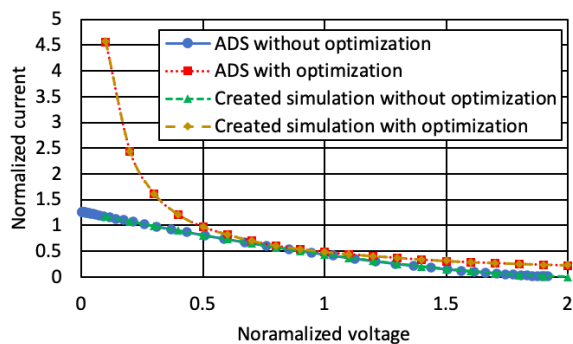


FIGURE 16. i-v of an ideal rectifier.

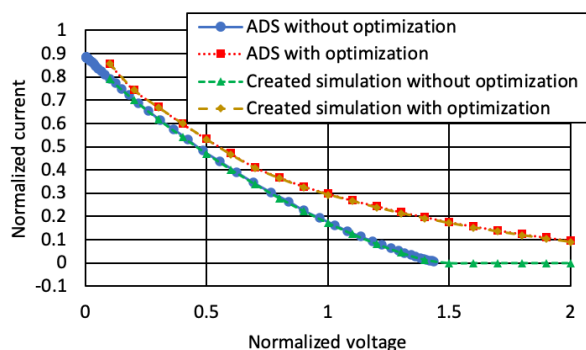


FIGURE 17. i-v with $R_s = 10 \Omega$, $C_j = 10^{-12} \text{ F}$ and $f = 2.45 \text{ GHz}$.

The optimized circuit is simulated by our program and ADS. Their results are compared in the following sections.

B. OPTIMIZED RECTIFIER

We conducted the simulations and optimizations. First, we simulated the ideal single shunt rectifier with our program. The output DC voltage was changed from 0.1 to 2.0 by 0.1 in these simulations. Fig. 16 shows the i-v characteristics of an ideal single shunt rectifier and that with the optimized input filters. The blue and green lines are the same as Fig. 13. Characteristics with the optimized stubs are shown by the red and yellow lines. These lines completely matched.

Next, we simulated the single shunt rectifier (Fig. 10) with the equivalent circuit (Fig. 15). We set the values $R_s = 10 \Omega$, $C_j = 10^{-12} \text{ F}$, and $f = 2.45 \text{ GHz}$. The output DC voltage is changed from 0.1 to 2.0 by 0.1 in these simulations. Fig. 17 shows the simulation results. The blue and green lines indicate i-v characteristics without any input filters and these lines have no differences. The red and yellow lines indicates i-v characteristics with the optimized input filters, and these lines are also completely matched. These results show the accuracy of our proposed method.

VI. CONCLUSION

This paper shows a novel analysis of the ideal single shunt rectifiers. First, we show the basic theories regarding wave propagation in the striplines. We revealed the basic characteristics of the stripline with a parallel connected diode. Next, we calculated the forms of incident and reflection waves to a

diode in an ideal single shunt rectifier. Calculating the average current, the theoretical i-v characteristics were revealed. As a result, our analysis shows the detail characteristics of an ideal single shunt rectifier and its operations. Results of analytical calculations and simulations are completely matched, and their maximum RF-DC conversion efficiencies of ideal single shunt rectifiers are 92.26 %. The ideal conditions of the output filter is also described from the time domain.

Next, we proposed a novel simulation method based on our theoretical analysis. This method can solve the DC current output from the output DC voltage. We compared the results from our program and commercial simulation ADS. They are completely matched, which shows that our simulation is consistent with existing simulations and physical characteristics of single shunt rectifiers. Our analytical method focuses on the transient phenomena. Therefore, our simulation has high affinity with time evolution simulation (for example, FDTD). In addition, this method enables the direct analysis of time variation coefficients such as junction capacitance. Proposed method uses the output DC voltage as a fixed parameter. This means our simulation is suitable for the conditions that an output voltage has little fluctuation, such that the load is a battery. In conclusion, we show the detailed operation of single shunt rectifiers and a novel analysis method.

REFERENCES

- [1] W. C. Brown, "The history of power transmission by radio waves," *IEEE Trans. Microw. Theory Techn.*, vol. 32, no. 9, pp. 1230–1242, Sep. 1984.
- [2] J.-H. Ou, S. Y. Zheng, A. S. Andrenko, Y. Li, and H.-Z. Tan, "Novel time-domain Schottky diode modeling for microwave rectifier designs," *IEEE Trans. Circuits Syst. I, Reg. Papers*, vol. 65, no. 4, pp. 1234–1244, Apr. 2018.
- [3] J. J. Nahas, "Modeling and computer simulation of a microwave-to-DC energy conversion element," *IEEE Trans. Microw. Theory Techn.*, vol. 23, no. 12, pp. 1030–1035, Dec. 1975.
- [4] G. Boyakhchyan, V. Vanke, S. Lesota, F. Maslovskiy, and V. Novitskiy, "Analytical calculation of a high-efficiency microwave rectifier employing a schottky-barrier diode," *Telecommun. And Radio Eng.*, vol. 37, no. 10, pp. 64–66, 1983.
- [5] R. J. Gutmann and J. M. Borrego, "Power combining in an array of microwave power rectifiers," *IEEE Trans. Microw. Theory Techn.*, vol. 27, no. 12, pp. 958–968, Dec. 1979.
- [6] T.-W. Yoo and K. Chang, "Theoretical and experimental development of 10 and 35 GHz rectennas," *IEEE Trans. Microw. Theory Techn.*, vol. 40, no. 6, pp. 1259–1266, Jun. 1992.
- [7] J. O. McSpadden, L. Fan, and K. Chang, "Design and experiments of a high-conversion-efficiency 5.8-GHz rectenna," *IEEE Trans. Microw. Theory Techn.*, vol. 46, no. 12, pp. 2053–2060, Dec. 1998.
- [8] J. Guo and X. Zhu, "An improved analytical model for RF-DC conversion efficiency in microwave rectifiers," in *IEEE MTT-S Int. Microw. Symp. Dig.*, Jun. 2012, pp. 1–3.
- [9] S. Imai, S. Tamaru, K. Fujimori, M. Sanagi, and S. Nogi, "Efficiency and harmonics generation in microwave to DC conversion circuits of half-wave and full-wave rectifier types," in *IEEE MTT-S Int. Microw. Symp. Dig.*, May 2011, pp. 15–18.
- [10] M. Roberg, T. Reveyrand, I. Ramos, E. A. Falkenstein, and Z. Popovic, "High-efficiency harmonically terminated diode and transistor rectifiers," *IEEE Trans. Microw. Theory Techn.*, vol. 60, no. 12, pp. 4043–4052, Dec. 2012.
- [11] J. Guo, H. Zhang, and X. Zhu, "Theoretical analysis of RF-DC conversion efficiency for Class-F rectifiers," *IEEE Trans. Microw. Theory Techn.*, vol. 62, no. 4, pp. 977–985, Apr. 2014.
- [12] S.-P. Gao, H. Zhang, and Y.-X. Guo, "Closed-form expressions based automated rectifier synthesis," in *IEEE MTT-S Int. Microw. Symp. Dig.*, May 2019, pp. 1–3.

- [13] S.-P. Gao, H. Zhang, T. Ngo, and Y. Guo, "Lookup-table-based automated rectifier synthesis," *IEEE Trans. Microw. Theory Techn.*, vol. 68, no. 12, pp. 5200–5210, Dec. 2020.
- [14] M. Nakhla and J. Vlach, "A piecewise harmonic balance technique for determination of periodic response of nonlinear systems," *IEEE Trans. Circuits Syst.*, vol. 23, no. 2, pp. 85–91, Feb. 1976.
- [15] A. Vladimirescu, *The SPICE Book*. New York, NY, USA: Wiley, 1994, pp. 169–179.



TAKASHI HIRAKAWA (Student Member, IEEE) received the B.S. degree in electrical and electronic engineering from Kyoto University, in 2016. Since 2016, he has been with the Electrical Engineering, Kyoto University, to study about microwave techniques.



NAOKI SHINOHARA (Senior Member, IEEE) received the B.E. degree in electronic engineering, and the M.E. and Ph.D. (Eng.) degrees in electrical engineering from Kyoto University, Japan, in 1991, 1993, and 1996, respectively. Since 1996, he has been a Research Associate with Kyoto University, where he has also been a Professor, since 2010. He has been involved in research on Solar Power Station/Satellite and Microwave Power Transmission system. He was an IEEE

MTT-S Distinguish Microwave Lecturer from 2016 to 2018. He is an IEEE MTT-S Technical Committee 25 (Wireless Power Transfer and Conversion) Former Chair, an IEEE MTT-S Kansai Chapter TPC member, the IEEE Wireless Power Transfer Conference founder, and an Advisory Committee Member, the URSI Commission D Vice Chair, the *International Journal of Wireless Power Transfer* (Cambridge Press) an Executive Editor, the First Chair, and a Technical Committee Member on IEICE Wireless Power Transfer, the Japan Society of Electromagnetic Wave Energy Applications Adviser, the Space Solar Power Systems Society Vice Chair, the Wireless Power Transfer Consortium for Practical Applications (WiPoT) Chair, and the Wireless Power Management Consortium (WPMc) Chair. His books are *Wireless Power Transfer via Radiowave* (ISTE Ltd., and John Wiley & Sons, Inc.), *Recent Wireless Power Transfer Technologies Via Radio Waves (ed.)* (River Publishers), and *Wireless Power Transfer: Theory, Technology, and Applications (ed.)* (IET), and some Japanese text books of WPT.

...